Cell Stem Cell
Article

SIRT1 Activation by a c-MYC Oncogenic Network Promotes the Maintenance and Drug Resistance of Human FLT3-ITD Acute Myeloid Leukemia Stem Cells

Ling Li,[1] Tereza Osdal,[2] Yinwei Ho,[1] Sookhee Chun,[1] Tinisha McDonald,[1] Puneet Agarwal,[1] Allen Lin,[1] Su Chu,[1] Jing Qi,[1] Liang Li,[1] Yao-Te Hsieh,[1] Cedric Dos Santos,[1] Hongfeng Yuan,[5] Trung-Quang Ha,[2] Mihaela Popa,[3] Randi Hovland,[7] Øystein Bruserud,[2,4] Bjørn Tore Gjertsen,[2,4] Ya-Huei Kuo,[1] Wenyong Chen,[5] Sonia Lain,[6] Emmet McCormack,[2,4,*] and Ravi Bhatia[1,*]

[1]Division of Hematopoietic Stem Cell and Leukemia Research, City of Hope National Medical Center, Duarte, CA 91010, USA
[2]Department of Clinical Science, Hematology Section, University of Bergen, Bergen 5021, Norway
[3]KinN Therapeutics AS, Bergen 5008, Norway
[4]Department of Internal Medicine, Hematology Section, Haukeland University Hospital, Bergen 5021, Norway
[5]Department of Cancer Biology, City of Hope National Medical Center, Duarte, CA 91010, USA
[6]Karolinska Institutet, Stockholm 17177, Sweden
[7]Center for Medical Genetics and Molecular Medicine, Haukeland University Hospital, Bergen 5021, Norway
*Correspondence: emmet.mc.cormack@k2.uib.no (E.M.), rbhatia@coh.org (R.B.)
http://dx.doi.org/10.1016/j.stem.2014.08.001

SUMMARY

The FLT3-ITD mutation is frequently observed in acute myeloid leukemia (AML) and is associated with poor prognosis. In such patients, FLT3 tyrosine kinase inhibitors (TKIs) are only partially effective and do not eliminate the leukemia stem cells (LSCs) that are assumed to be the source of treatment failure. Here, we show that the NAD-dependent SIRT1 deacetylase is selectively overexpressed in primary human FLT3-ITD AML LSCs. This SIRT1 overexpression is related to enhanced expression of the USP22 deubiquitinase induced by c-MYC, leading to reduced SIRT1 ubiquitination and enhanced stability. Inhibition of SIRT1 expression or activity reduced the growth of FLT3-ITD AML LSCs and significantly enhanced TKI-mediated killing of the cells. Therefore, these results identify a c-MYC-related network that enhances SIRT1 protein expression in human FLT3-ITD AML LSCs and contributes to their maintenance. Inhibition of this oncogenic network could be an attractive approach for targeting FLT3-ITD AML LSCs to improve treatment outcomes.

INTRODUCTION

Acute myeloid leukemia (AML) is organized as a hierarchy with small populations of self-renewing leukemic stem cells (LSCs) generating the bulk of leukemic cells (Patel et al., 2012). LSCs can resist elimination by conventional therapy and persist as potential sources of relapse. Several studies indicate that LSC gene expression signatures are correlated with poor prognosis in AML patients (Eppert et al., 2011). Better understanding of LSC regulation is critical for developing improved therapies against AML.

Internal tandem duplications (ITDs) in the Fms-like tyrosine kinase (FLT3) are seen in 25%–30% of AML patients, constituting the most commonly observed mutation in AML (Kindler et al., 2010). FLT3-ITD is associated with reduced length of remission and survival, consistent with lack of elimination of LSC (Kindler et al., 2010; Horton and Huntly, 2012). The ITD mutation results in constitutive FLT3 activation and altered downstream signaling compared to wild-type (WT) FLT3 (Nakao et al., 1996). In animal models, expression of FLT3-ITD alone results in a myeloproliferative disorder, and cooperating mutations are required for AML development (Chu et al., 2012). Several small molecule FLT3 tyrosine kinase inhibitors (TKIs), such as quizartinib (AC220), are being examined (Levis, 2011; Smith et al., 2012). However, FLT3-TKIs only partially inhibit human FLT3-ITD AML LSCs and demonstrate modest clinical activity (Horton and Huntly, 2012; Levis, 2011; Smith et al., 2012). Resistance can emerge during treatment through point mutations that interfere with drug binding (Smith et al., 2012). Better understanding of molecular events contributing to the drug resistance of FLT3-ITD LSC would aid development of approaches to achieve sustained remissions.

The NAD-dependent deacetylase sirtuin 1 (SIRT1) modulates the activity of several intracellular proteins, including p53 (Vaziri et al., 2001). SIRT1 regulates numerous cellular processes including aging, DNA repair, cell cycle, metabolism, and survival (Brooks and Gu, 2009). SIRT1 plays an important role in maintaining self-renewal and differentiation of murine embryonic stem cells and hematopoietic stem cells (HSCs), especially under conditions of stress (Han et al., 2008; Ou et al., 2011). Several studies indicate a pathogenic role for SIRT1 in solid tumors and leukemias (Brooks and Gu, 2009). However, other studies suggest tumor-suppressive functions (Wang et al., 2008a, 2008b), implying that the role of SIRT1 in cancer may be context dependent, varying by the tumor type, specific oncogenes present, and mutation status of p53 or other target proteins (Brooks and Gu, 2009). We have reported that SIRT1 is overexpressed in chronic myeloid leukemia (CML) LSCs and that SIRT1 inhibition selectively eliminates CML LSCs by

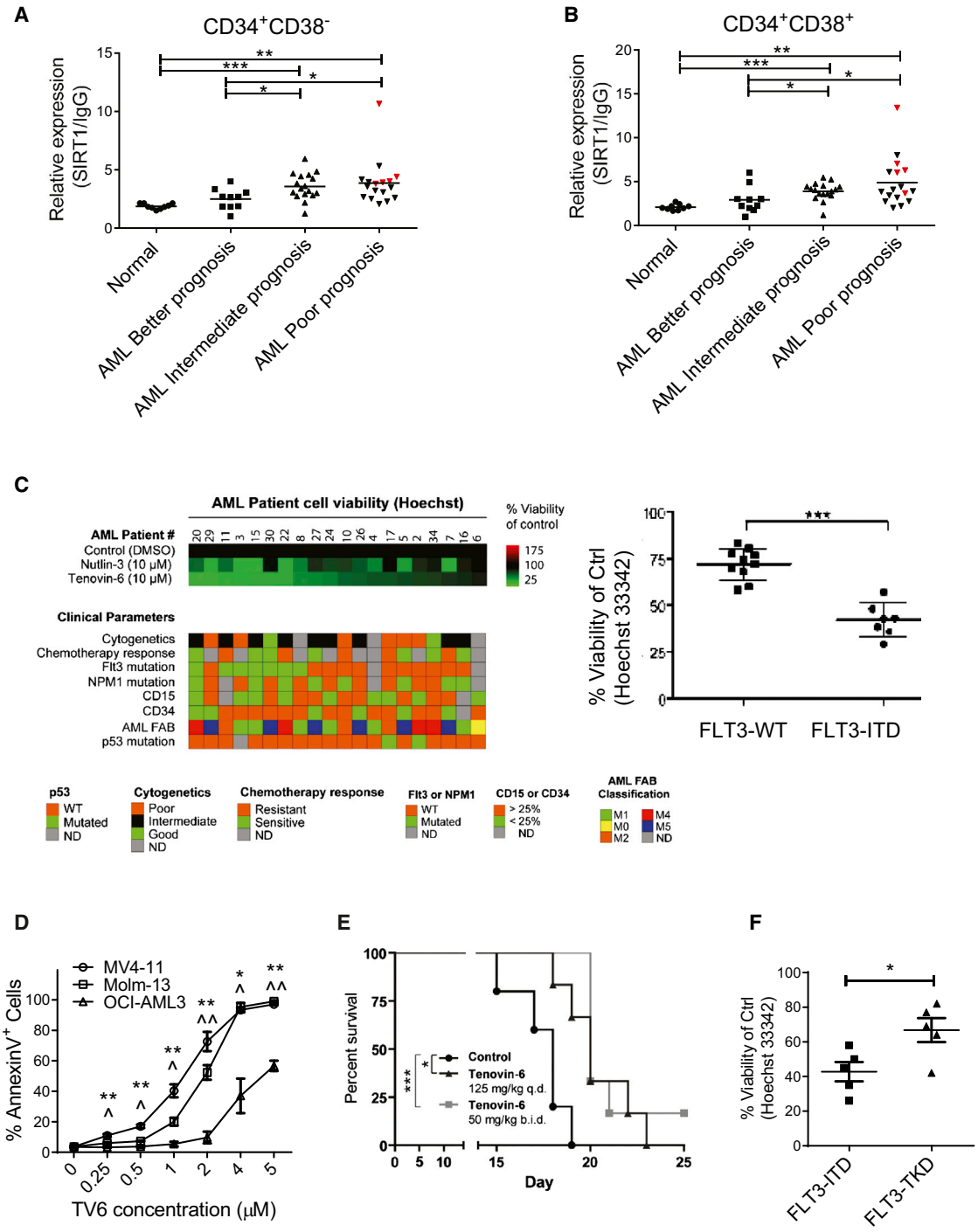

Figure 1. SIRT1 Expression and Sensitivity to TV6 in AML Compared with Normal Stem/Progenitor Cells

(A and B) SIRT1 protein expression in $CD34^+CD38^-$ (A) and $CD34^+$ $CD38^+$ (B) cells from better risk (n = 10), intermediate-risk (n = 17) and poor-risk (n = 17) AML and normal CB and PBSC samples was analyzed by flow cytometry. Median fluorescence intensity of SIRT1 was expressed relative to that of immunoglobulin G (IgG) control. FLT3-ITD AML samples are indicated in red.

(C) Sensitivity of AML samples (n = 20) to TV6 (10 μM) and nutlin-3 (10 μM) treatment for 24 hr. Viability was tested using Hoechst 33342 staining. Clinical and genetic parameters for individual samples are shown. Flt3 mutation indicates FLT3-ITD mutation.

(D) Effect of 48 hr TV6 treatment on apoptosis of WT p53 FLT3-ITD MV4-11 and Molm-13 AML cells, and on FLT3-WT OCI-AML3 cells, using annexin V/DAPI staining. Results represent mean ± SEM of three separate experiments. *p < 0.05 and **p < 0.01 for MV4-11 versus OCI-AML3; ^p < 0.05 and ^^p < 0.01 for Molm-13 versus OCI-AML3.

(legend continued on next page)

increasing p53 acetylation and activity (Li et al., 2012). Although the role of SIRT1 in murine adult HSCs is controversial (Leko et al., 2012; Singh et al., 2013), SIRT1 inhibition has only a minor impact on normal human CD34$^+$ hematopoietic cells (Li et al., 2012; MacCallum et al., 2013).

Given the association of SIRT1 activation with BCR-ABL (Yuan et al., 2012) and the reported sensitivity of FLT3-ITD AML samples to p53-activating drugs (Long et al., 2010; McCormack et al., 2012), we were interested in evaluating whether the FLT3-ITD kinase was also associated with increased SIRT1 expression and activity. We studied SIRT1 expression and effects of SIRT1 inhibition in a large group of human AML samples from two centers. We evaluated the association between FLT3-ITD and increased SIRT1 activity, as well as the contribution of SIRT1 to survival, growth, and TKI response of FLT3-ITD AML LSC. Finally, we investigated mechanisms contributing to SIRT1 activation in FLT3-ITD AML.

RESULTS

SIRT1 Overexpression and Sensitivity to SIRT1 Inhibition in AML CD34$^+$ Cells

We measured SIRT1 protein levels in AML and normal cord blood (CB) and PB stem cell (PBSC) CD34$^+$CD38$^+$ committed progenitors and CD34$^+$CD38$^-$ primitive progenitors by labeling with anti-SIRT1 antibody and flow cytometry (Li et al., 2012). The majority of AML CD34$^+$CD38$^-$ cells (n = 44) showed increased SIRT1 expression compared to normal samples (Figure 1A). SIRT1 expression was also increased in AML compared to normal CD34$^+$CD38$^+$ cells (Figure 1B). SIRT1 levels were higher in cells from patients with poor and intermediate, compared with better risk, genetic lesions based on National Cancer Center Network (NCCN) criteria (O'Donnell et al., 2012) (Figure 1A). Since SIRT1 can deacetylate and inhibit p53 activity (Vaziri et al., 2001; Li et al., 2012), we evaluated the effect of the SIRT1 inhibitor Tenovin-6 (TV6; 10 μM) and the MDM2 antagonist nutlin-3 (10 μM) on the viability of AML cells. TV6 and nutlin-3 demonstrated similar efficacy, on average, in inhibiting the viability of AML blasts (Figure S1A available online). As expected, moderate sensitivity to TV6 was seen in p53 wild-type (WT) samples (n = 25) but not p53 mutant samples (n = 5) (Figure S1B). On the other hand, individual AML samples showed discrepancies between TV6 and nutlin-3 sensitivity, suggesting that additional factors may influence sensitivity. In samples showing >20% difference in viability after TV6 and nutlin-3 treatment, the FLT3-ITD mutation was associated with increased TV6 sensitivity ($p < 0.001$) (Figure S1D). We also observed increased representation of FLT3-ITD in AML samples with the highest sensitivity to TV6 (7 of 20 samples, $p < 0.001$) (Figure 1C), and in AML CD34$^+$CD38$^-$ and CD34$^+$CD38$^+$ cells with the highest SIRT1 expression (Figures 1A and 1B). The Molm-13 and MV4-11 AML cell lines (p53 WT and FLT3-ITD$^+$) showed significantly increased sensitivity to TV6 compared with FLT3 WT (FLT3-WT) and p53 WT OCI-AML3 cells; FLT3-WT and p53 null HL-60 cells; and FLT3-WT and p53 mutant NB4 cells (Figures 1D and S1C). TV6 treatment significantly decreased leukemic burden and prolonged survival of mice xenografted with luciferase expressing Molm-13 cells (McCormack et al., 2012) (Figures 1E, S1E, and S1F). Moreover, TV6 significantly decreased the leukemic burden in mice engrafted with control small hairpin RNA (shRNA) but not p53 shRNA-expressing Molm13 cells (Figure S1G). FLT3 tyrosine kinase domain (TKD) mutations (D835Y) are also seen in 5% of AML cases (Kindler et al., 2010). It is interesting that FLT3-TKD samples were significantly less sensitive to TV6 compared to FLT3-ITD samples (Figure 1F). Cumulatively, these data suggest that the FLT3-ITD mutation identifies AML cells with increased sensitivity to SIRT1 inhibition.

Increased SIRT1 Expression and Sensitivity to SIRT1 Knockdown in FLT-ITD$^+$ AML CD34$^+$ cells

We further demonstrated that SIRT1 protein levels were significantly increased in FLT3-ITD (n = 8) compared to FLT3-WT (n = 9) or FLT3-TKD (n = 5) AML CD34$^+$ cells (Figure 2A). SIRT1 expression was increased in FLT3-ITD compared to FLT3-WT AML CD34$^+$CD38$^-$ cells (n = 4, each group) coexpressing two well-described LSC markers, CD47 (Majeti et al., 2009) and CD123 (Jordan et al., 2000) (Figure S2A). SIRT1 expression in FLT3-ITD AML samples was highest in S/G2/M, followed by G1 and then G0 phase (data not shown). CB CD34$^+$ cells transduced with FLT3-ITD-expressing lentivirus vectors showed increased SIRT1 and reduced acetylated p53 levels compared to FLT3-WT or control vectors (Figures 2B and S2B). On the other hand, significant differences in SIRT1 messenger RNA (mRNA) levels were not seen between FLT3-ITD and FLT3-WT AML CD34$^+$ cells (Figure 2C), or between CB CD34$^+$ cells expressing FLT3-ITD and FLT3-WT genes (data not shown). SIRT1 protein half-life was increased in FLT3-ITD MV4-11 cells treated with cyclohexamide (CHX) to inhibit translation, compared to FLT3-WT OCI-AML3 cells (Figure S2C), and in CD34$^+$ cells ectopically expressing FLT3-ITD compared to FLT3-WT (Figure 2D). These results suggest that increased SIRT1 expression in FLT3-ITD AML cells is related to increased protein stability.

Since SIRT1-mediated deacetylation can inhibit p53 activity, we analyzed p53 target gene induction after γ-irradiation (3 Gy, 6 hr) in FLT3-ITD and FLT3-WT AML CD34$^+$ cells (all with WT p53 by sequencing). We observed reduced induction of mRNA for p53 target genes, especially *BAX* and *NOXA*, in FLT3-ITD compared to FLT3-WT cells (Figure 2E). FLT3-ITD MV4-11 cells showed reduced radiation-induced increase in p21, BAX, NOXA, PUMA, and DR5 protein levels compared to FLT3-WT OCI-AML3 cells (Figure S2D). Knockdown of BAX using small interfering RNA (siRNA) significantly reduced radiation-induced apoptosis in MV4-11 cells and OCI-AML3 (Figures S2E and

(E) Survival of NSG mice transplanted with MOLM-13luc cells and treated starting 5 days later with TV6 intraperitoneally (125 mg/kg daily or 50 mg/kg twice a day) for 12 days. Survival of mice treated with both TV6 regimens was significantly longer than controls ($p < 0.05$ for 125 mg/kg once daily; $p < 0.001$ for 50 mg/kg twice daily).

(F) Sensitivity of AML samples with WT p53, FLT3-ITD (n = 5), or FLT3-TKD (n = 5) mutations to TV6 (10 μM) for 24 hr. Viability was tested using Hoechst 33342 staining.

*$p < 0.05$, **$p < 0.01$, and ***$p < 0.001$. See also Figure S1 and Tables S1, S2, and S3.

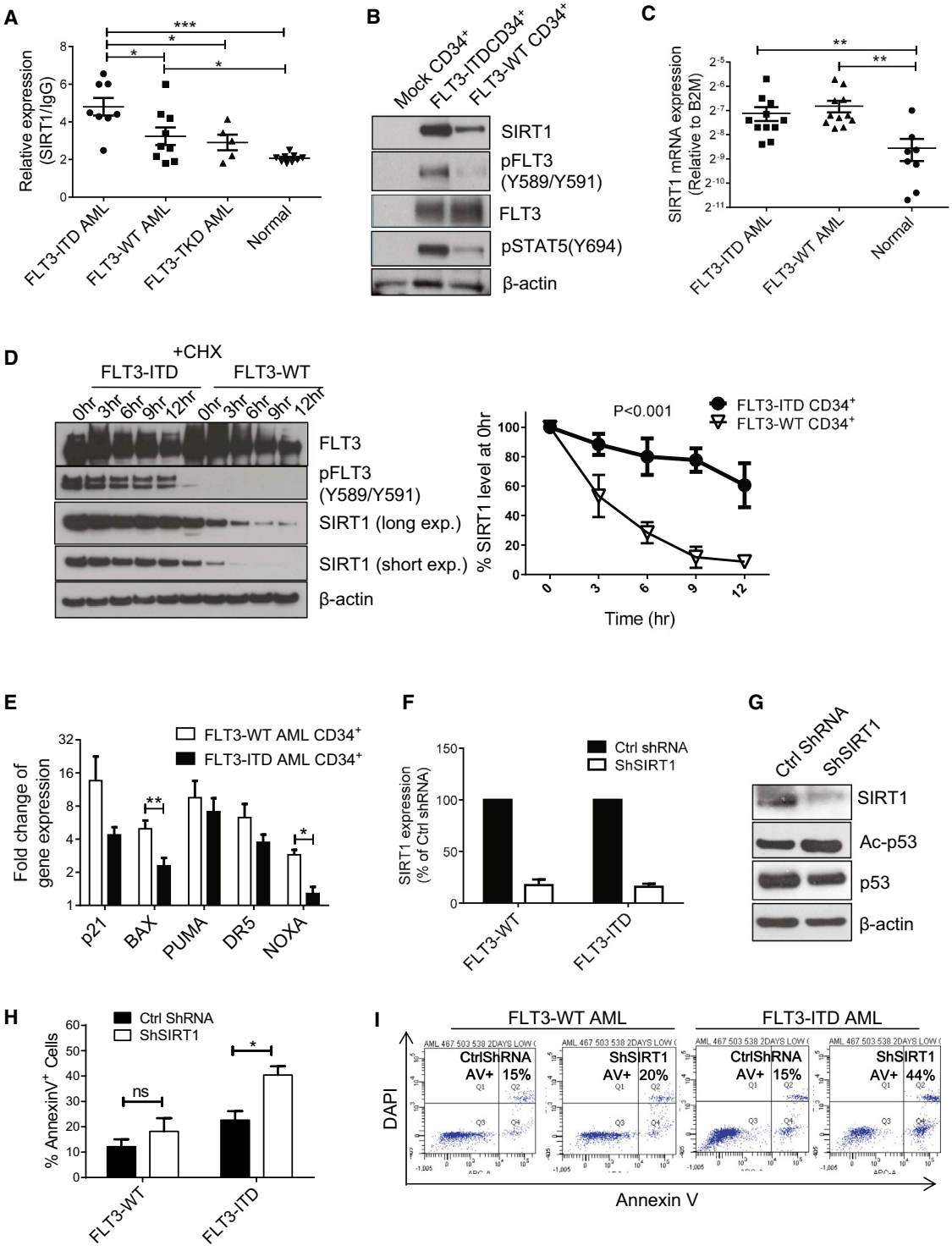

Figure 2. Increased SIRT1 Expression and Sensitivity to SIRT1 Knockdown in FLT-ITD$^+$ AML CD34$^+$ Cells

(A) SIRT1 protein expression in CD34$^+$ cells from FLT3-ITD AML (n = 8), FLT3-WT AML (n = 9), FLT-TKD AML (n = 5), and normal CB or PBSC (n = 9) samples analyzed by intracellular flow cytometry. IgG, immunoglobulin G.

(B) Western blotting for SIRT1, FLT3, p-FLT3 (Y589/Y591), p-STAT5 (Y694), and β-actin in CB CD34$^+$ cells transduced with vectors expressing green fluorescent protein (GFP) alone (Mock), FLT3-ITD, or FLT3-WT. Results are representative of three experiments.

(C) SIRT1 mRNA expression in CD34$^+$ cells from FLT3-ITD (n = 11), FLT3-WT AML (n = 11), CB or normal PBSC (n = 8) samples analyzed by quantitative PCR.

(D) Western blotting for SIRT1, FLT3, pFLT3 (Y589/Y591), and β-actin in FLT3-ITD or FLT3-WT expressing CD34$^+$ cells treated with CHX. The right panel indicates the relative amount of SIRT1 analyzed by densitometry (n = 3). exp., exposure.

(legend continued on next page)

S2F), indicating its importance as an effector of p53 response. Radiation-induced apoptosis of MV4-11, but not OCI-AML3, cells was significantly increased by TV6 pretreatment, and this effect was also prevented by BAX knockdown (Figure S2F).

To further evaluate the functional role of SIRT1 in modulating p53 function in FLT3-ITD AML CD34$^+$ cells, we inhibited SIRT1 expression using lentivirus vectors expressing SIRT1 shRNA (ShSIRT1) (Figures 2F and 2G) (Li et al., 2012). SIRT1 knockdown increased acetylated p53 levels (Figure 2G) and significantly increased apoptosis of FLT3-ITD cells ($p < 0.05$) but not FLT3-WT AML CD34$^+$ cells (Figures 2H and 2I) or normal CD34$^+$ cells (Figure S2G). These results suggest that SIRT1 deacetylates p53 and inhibits p53 signaling to maintain survival of FLT3-ITD AML progenitors. Since SIRT2 is also targeted by TV6 and could also regulate AML cell growth (Dan et al., 2012), we compared effects of anti-SIRT1 and anti-SIRT2 shRNA in FLT3-ITD (MV4-11, Molm-13) and FLT3-WT (OCI-AML3) AML cells (Figures S2H–S2J). Whereas SIRT1 knockdown significantly reduced survival and proliferation of the two FLT3-ITD cell lines but not the FLT3-WT line, SIRT2 knockdown did not affect survival and proliferation of FLT3-ITD AML cells, suggesting a less critical role. To further exclude off-target effects of ShSIRT1, we expressed a ShSIRT1-resistant SIRT1 construct (PITA-SIRT1-R) containing five silent mutations in the shRNA-targeted region in MV4-11 cells (Li et al., 2012). Expression of SIRT1-R maintained SIRT1 protein levels after ShSIRT1 transduction (Figure S2K) and abrogated the ability of ShSIRT1 to inhibit growth (Figure S2L), suggesting that ShSIRT1 effects are indeed related to SIRT1 knockdown.

Pharmacological Inhibition of SIRT1 Inhibits AML Progenitors

TV6 significantly enhanced acetylated and total p53 levels in FLT3-ITD AML CD34$^+$ cells (Figure 3A, left panel; Figure S3A). Cells pretreated with nutlin-3 to stabilize p53 levels showed a dose-dependent increase in p53 acetylation after TV6 treatment, with minimal change in total p53 levels, indicating that increased p53 acetylation was independent of increase in total p53 (Figure 4C and Figure S3C). TV6 did not increase acetylated or total p53 in FLT3-WT AML CD34$^+$ cells, whereas nutlin-3 increased total p53 levels (Figure 3A, right panel; Figure S3B). In p53 null K562 cells ectopically expressing WT p53 protein, TV6 increased p53 acetylation without changing total p53 levels (Figure S3D). In contrast, in K562 cells ectopically expressing a p53 mutant with eight potential acetylation sites mutated (p53-8KR), TV6 failed to increase p53 acetylation and resulted in significantly less apoptosis ($p < 0.01$) (Figure S3E), confirming the importance of p53 acetylation for inhibitory effects of TV6. The proliferation inhibitory effects of TV6 were significantly reduced following SIRT1 knockdown in MV4-11 cells, further indicating the importance of SIRT1 expression for TV6 effects (Figure S3F). TV6 also increased expression of mRNA for the p53 target genes *p21*, *BAX*, *PUMA*, *NOXA*, and *DR5* ($p < 0.05$) in FLT3-ITD AML CD34$^+$ cells (Figure 3B). shRNA-mediated knockdown of p53 significantly reduced TV6 or SIRT1 knockdown-induced growth inhibition in FLT3-ITD cells (Figures 3C, 3D, S3G, and S3H), supporting an important role for p53 in SIRT1-mediated effects. TV6 treatment resulted in increased inhibition of survival (Figure 3E) and proliferation (Figure 3F) of FLT3-ITD compared to FLT3-WT AML CD34$^+$ cells and normal CD34$^+$ cells ($p < 0.05$). Similarly, CB CD34$^+$ cells ectopically expressing FLT3-ITD showed increased sensitivity to TV6-mediated apoptosis (Figure 3G) and growth inhibition (Figure 3H), compared to FLT3-WT- or vector-transduced CD34$^+$ hematopoietic cells.

SIRT1 Inhibition Enhances AC220-Mediated Inhibition on FLT3-ITD AML Progenitors

Knockdown of FLT3 expression in AML CD34$^+$ cells only modestly decreased SIRT1 expression (Figure 4A). Similarly, the FLT3 TKI AC220, despite effectively inhibiting FLT3 kinase activity in FLT3-ITD AML CD34$^+$ cells (Figures 4B and S4A), only partially decreased SIRT1 and p53 levels without significantly affecting p53 acetylation (Figures 4C and S4A) or p53 target gene expression (Figure S4B). These results indicate that FLT3 inhibition only marginally affects SIRT1-p53 signaling in FLT3-ITD AML cells. TV6 alone did not significantly affect FLT3 signaling, as evidenced by pSTAT5 expression (Figures 4B and 4C). TV6 increased acetylated p53 expression (Figure 4C) and enhanced p53 target gene expression in AC220-treated FLT3-ITD AML CD34$^+$ cells (Figure 4D). SIRT1 knockdown using shRNA also increased acetylated p53 expression in AC220-treated FLT3-ITD AML cells (Figure S4C). AC220-induced apoptosis and growth inhibition of MV4-11 cells was significantly enhanced by combination of AC220 with TV6 (Figures S4D and S4E). Consistent with previous reports (Levis, 2011), AC220 only modestly inhibited survival of primary human FLT3-ITD AML CD34$^+$ cells (Figure 4E). The combination of TV6 (1 μM) with AC220 (20nM) significantly reduced the survival, growth, and colony-forming capacity of FLT3-ITD AML CD34$^+$ cells compared to AC220 or TV6 alone (Figures 4E–4G). ShSIRT1 in combination with AC220 also enhanced inhibition of AML cell survival, growth, and colony formation compared to AC220 alone (Figures 4H–4J). These findings indicate that SIRT1 inhibition enhances targeting of FLT3-ITD AML progenitors in combination with TKI.

TV6 Enhances Targeting of FLT3-ITD LSCs In Vivo in Combination with TKI

We tested the in vivo effect of TV6, AC220, and the combination of both on primary human cells from three FLT3-ITD AML samples engrafted in NOD *scid* gamma (NSG) mice (Figure 5A). Following confirmation of engraftment in peripheral blood (PB) (>5% human CD45$^+$ cells), mice were treated with either vehicle (control), AC220 (10 mg/kg, gavage), TV6 (100 mg/kg,

(E) Expression of p53 target genes in FLT3-ITD (n = 11) and FLT3-WT (n = 9) AML CD34$^+$ cells 6 hr after irradiation (3 Gy) compared with nonirradiated control cells. (F–I) ShSIRT1 and control shRNA (Ctrl ShRNA) were expressed in FLT3-ITD AML cells. (F) SIRT1 mRNA expression in ShSIRT1- and control-shRNA-expressing AML CD34$^+$ cells (n = 3 per group). (G) SIRT1, acetylated p53 (Ac-p53), total p53, and β-actin levels in SIRT1- or control-shRNA-transduced MV4-11 AML cells analyzed by western blotting. (H) Apoptosis of FLT3-ITD (n = 5) and FLT3-WT (n = 5) AML CD34$^+$ cells expressing control and SIRT1 shRNA. Representative fluorescence-activated cell sorting plots are shown in (I).
Results represent mean ± SEM. *$p < 0.05$, **$p < 0.01$, and ***$p < 0.001$. See also Figure S2.

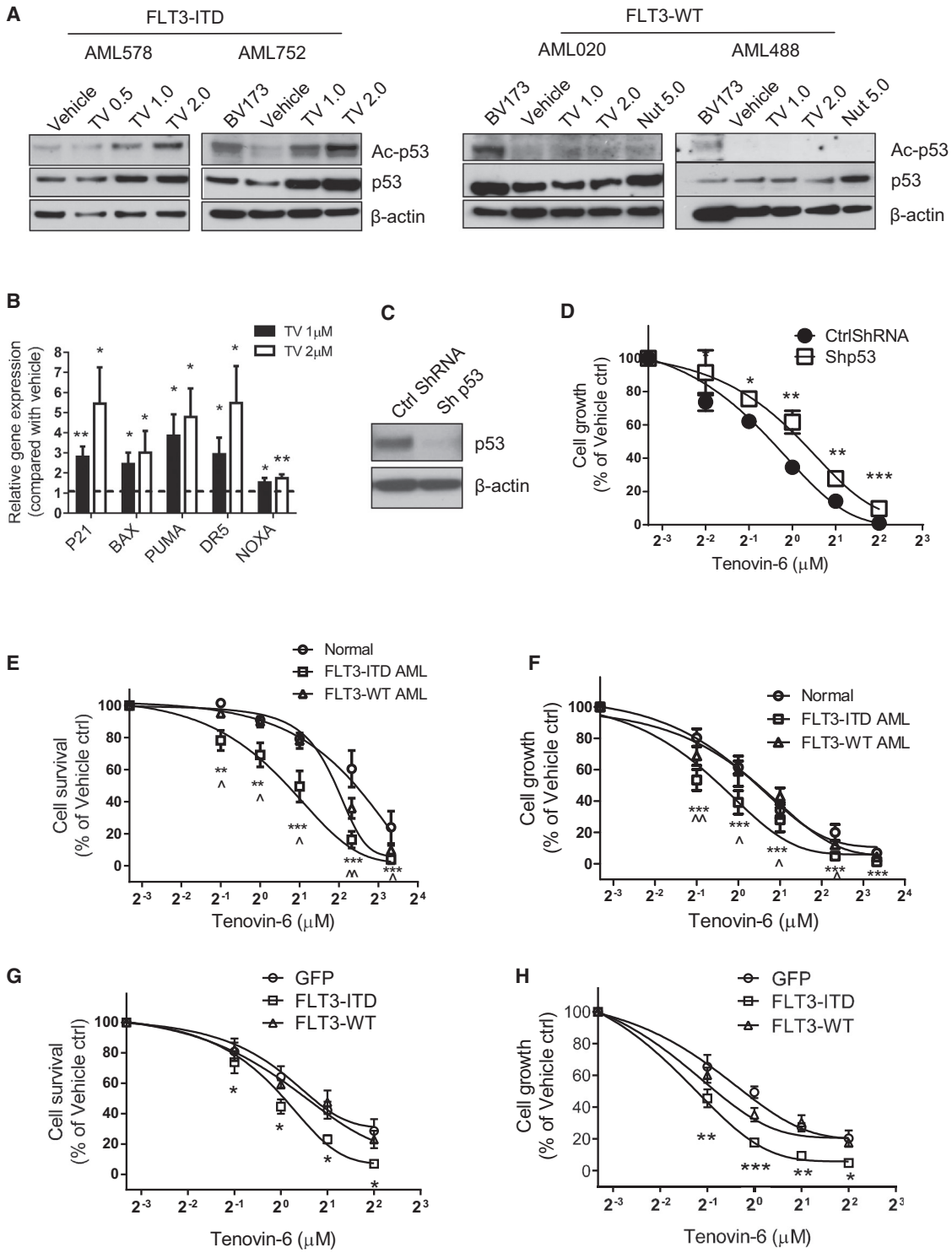

Figure 3. Inhibition of SIRT1 by TV6 Reduces FLT3-ITD AML CD34$^+$ Cell Growth and Survival by Activating p53 Signaling

(A) Western blotting for acetylated p53 (K382), total p53, and β-actin in FLT3-ITD (left panel) or FLT3-WT (right panel) AML CD34$^+$ cells treated with TV6 or nutlin-3 at indicated doses (μM) for 8 hr. Results from two representative FLT3-ITD samples (out of five) and two representative FLT3-WT samples (out of five) are shown. BV173 cells were included to identify p53 bands.

(B) p53 target gene expression in TV6 compared with vehicle-treated FLT3-ITD AML CD34$^+$ cells analyzed by real-time quantitative RT-PCR (n = 7).

(C and D) p53 shRNA (Sh p53) or control shRNA (Ctrl ShRNA) were expressed in MV4-11 cells. (C) Western blotting for p53. (D) Growth of cells exposed to TV6 for 72 hr analyzed by CellTiter-Glo. *p < 0.05, **p < 0.01, ***p < 0.001, compared with control shRNA.

(legend continued on next page)

intraperitoneal), or the combination for 4 weeks, after which human leukemia cell engraftment in BM and spleen was analyzed by flow cytometry. Engrafted leukemic cells were $CD45^+$ and $CD33^+$ with variable CD14 and CD15 expression and expressed the FLT3-ITD gene (data not shown). TV6 or AC220 treatment reduced the percentage and total number of human leukemic cells in murine BM (Figures 5B, 5C, and S5A). The combination of TV6 and AC220 significantly reduced AML cell engraftment compared with AC220 alone (Figures 5B and S5A). Human $CD34^+$ cells in BM were significantly reduced in mice treated with TV6 or AC220 alone, with further reduction seen in the combination (Figure S5B). We observed treatment effects with the combination on the percentage and number of AML cell in the spleen and PB that were similar to those in BM cells of NSG mice (Figures S5C and S5D; data not shown). Secondary transplantation of BM cells from mice receiving combination treatment resulted in significantly reduced engraftment in PB at 8 and 16 weeks (Figure 5D) and in BM at 16 weeks (Figures 5E and S5E) compared to AC220 treatment alone, indicating reduced LSC capacity of residual cells. We also studied another sample from a chemotherapy-refractory AML patient using molecular imaging of primary patient xenografts with fluorescently labeled monoclonal antibodies, as described previously (McCormack et al., 2013). We observed significant differences between combination and single-arm groups after 4 weeks of therapy (combination versus TV6, $p = 0.0005$; combination versus AC220, $p = 0.015$) (Figures 5F and 5G). AC220 or combination treatment also resulted in significant reduction in splenomegaly (Figure S5F). Mice treated with TV6 demonstrated significantly improved survival after discontinuation of treatment compared to control mice ($p = 0.02$), and the combination of TV6 and AC220 further increased survival compared to AC220 alone ($p = 0.0153$) (Figure 5H). We also observed significantly enhanced survival after secondary transplantation of BM from mice receiving combination treatment (versus AC220, $p = 0.03$, $n = 3$) (Figure 5I). The combination of AC220 and TV6 significantly improved survival compared with AC220 ($p = 0.0034$) and standard chemotherapy ($p = 0.006$) (Figure S5G). These results show that the combination of AC220 and TV6 enhances targeting of primitive human AML LSC in vivo.

Cross-Regulation of SIRT1 and MYC in FLT3-ITD AML Cells

Since previous studies have shown an association between c-MYC and increased SIRT1 protein expression (Menssen et al., 2012), we evaluated the role of c-MYC in increased SIRT1 expression in FLT3-ITD AML. Analysis of two large AML gene expression data sets available through the Gene Expression Omnibus (GSE1159: FLT3-ITD AML [n = 73] versus FLT3-WT AML [n = 178] [Valk et al., 2004] and GSE8043: FLT3-ITD AML [n = 120] versus FLT3-WT AML [n = 291] [Bullinger et al., 2008]) showed significant enrichment of a c-MYC-related gene set in FLT3-ITD compared to FLT3-WT AML samples (Figure 6A). c-MYC activity in AML cells was measured using a lentivirus-expressed c-MYC reporter expressing firefly luciferase under control of a minimal CMV promoter and tandem repeats of the E box transcriptional response element. We confirmed that shRNA-mediated inhibition of c-MYC expression reduced luciferase activity in MV4-11 cells (Figure S6A). AC220 treatment inhibited reporter activity (Figure 6B), suggesting that c-MYC is regulated, at least in part, by FLT3-ITD kinase activity, which is consistent with previous reports (Kim et al., 2007). FLT3-ITD kinase may regulate c-MYC through STAT5-induced enhancement of PIM kinases (Choudhary et al., 2009), which can modulate c-MYC stability and activity via phosphorylation (van der Lugt et al., 1995). This is supported by the observation that FLT3-ITD $CD34^+$ cells showed higher PIM activity compared to cells expressing FLT3-WT, indicated by increased expression of the PIM targets including p-BAD (Ser112), p-4EBP1 (Thr37/46), and p-c-MYC (Ser62) (Figure 6C); and by the observation that siRNA-mediated inhibition of PIM1, but not PIM2, expression resulted in significantly decreased p-c-MYC (Ser62), c-MYC, and SIRT1 expression in MV4-11 cells (Figure 6D). AC220 treatment reduced c-MYC Ser62 phosphorylation and total c-MYC levels in MV4-11 cells (Figure S6B) and also reduced c-MYC levels in FLT3-ITD AML $CD34^+$ cells (Figures 6E and S6B).

To evaluate the role of c-MYC in regulating SIRT1 expression, we inhibited c-MYC expression in FLT3-ITD AML cells using c-MYC shRNAs (Sh c-MYC-1 and Sh c-MYC-2). c-MYC knockdown reduced SIRT1 protein expression in MV4-11 cells (Figure 6F). Similarly c-MYC siRNA reduced SIRT1 protein levels in FLT3-ITD AML $CD34^+$ cells (Figure 6G). Since SIRT1 protein half-life is increased in FLT3-ITD cells, we evaluated whether c-MYC regulated SIRT1 protein stability. We observed that shRNA-mediated inhibition of c-MYC expression led to accelerated reduction in SIRT1 levels in AML cells following CHX treatment (Figure 6H). Proteasome inhibition by PS341 enhanced SIRT1 expression in c-MYC knockdown cells (Figure S6C). We next evaluated the role of c-MYC in regulating SIRT1 ubiquitination by cotransfecting hemagglutinin (HA)-ubiquitin, Flag-SIRT1, and c-MYC into human embryonic kidney 293 (HEK293) cells; immunoprecipitating SIRT1 using an anti-FLAG antibody; and detecting ubiquitination by western blotting with an anti-HA antibody (Menssen et al., 2012). Coexpression of c-MYC significantly inhibited polyubiquitination of SIRT1 (Figure 6I). These findings indicate that c-MYC enhances SIRT1 expression by reducing ubiquitination and increasing protein stability.

We further assessed the reciprocal role of SIRT1 in regulating c-MYC in FLT3-ITD AML cells. SIRT1-mediated acetylation of c-MYC has been associated with increased stability and activity via altered proteasomal degradation or indirectly by altered

(E and F) FLT3-ITD AML (n = 11), FLT3-WT AML (n = 11), and normal PBSC (n = 4) $CD34^+$ cells were exposed to TV6 for 48 hr. (E) Cell survival was analyzed by annexin V labeling. (F) Cell growth was evaluated using the CellTiter Glo assay. $^{**}p < 0.01$, and $^{***}p < 0.001$, compared with untreated controls; $^{\wedge}p < 0.05$, and $^{\wedge\wedge}p < 0.01$, compared with normal PBSCs.

(G and H) CB $CD34^+$ cells transduced with vectors expressing GFP alone, FLT3-ITD, or FLT3-WT (n = 5 each) were exposed to TV6 for 48 hr. (G) Cell survival was analyzed by annexin V labeling. (H) Cell growth was evaluated using the CellTiter Glo assay. $^{*}p < 0.05$, $^{**}p < 0.01$, $^{***}p < 0.001$, compared with GFP-transduced cells.

Error bars represent mean ± SEM. See also Figure S3.

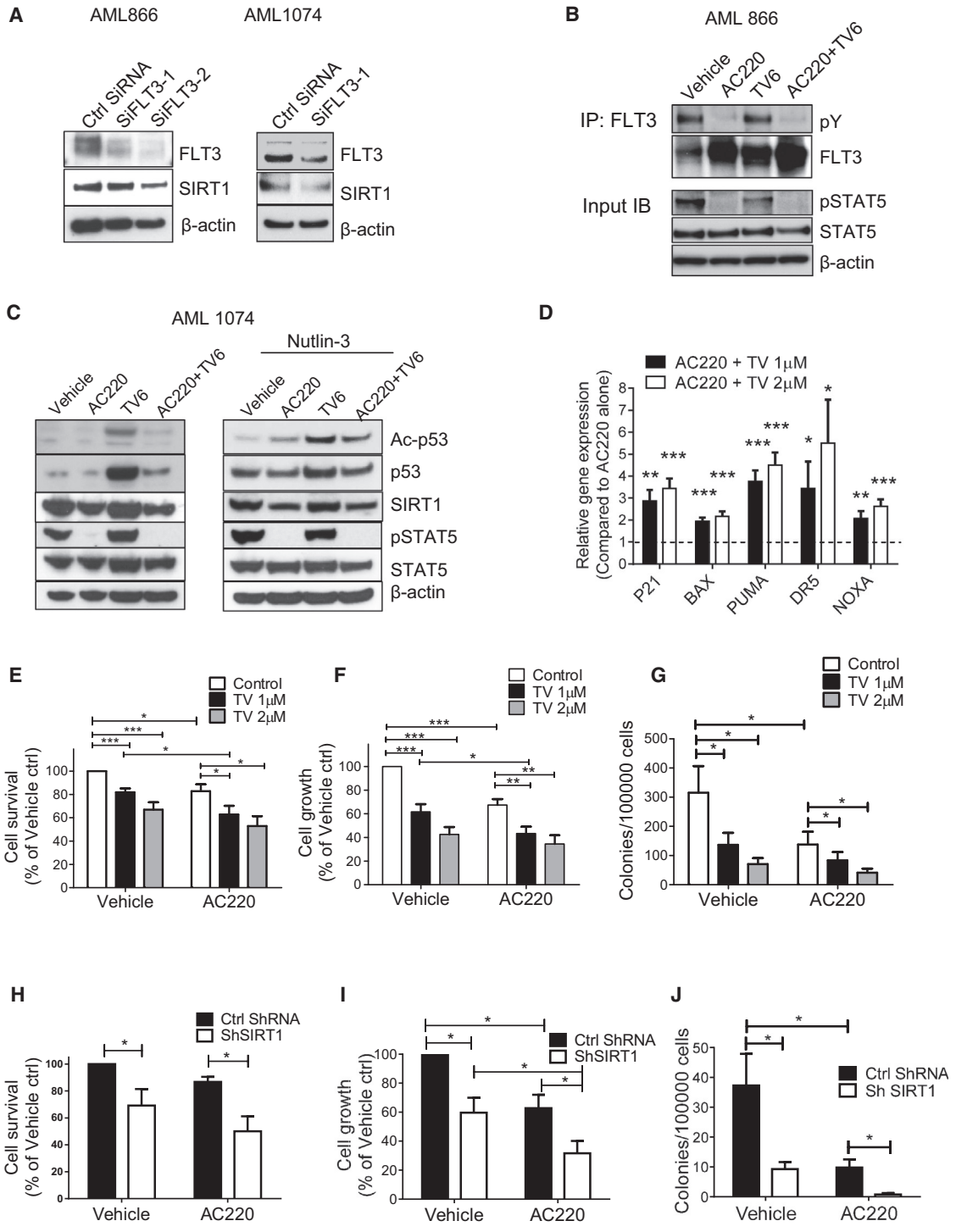

Figure 4. SIRT1 Inhibition Enhances AC220-Mediated Inhibition of FLT3-ITD AML CD34+ Cells

(A) Western blotting for FLT3, SIRT1, and β-actin in FLT3-ITD AML cells transfected with FLT3 siRNA and control siRNA (Ctrl SiRNA).

(B) FLT3 immunoprecipitates from FLT3-ITD AML CD34$^+$ cells exposed to TV6 (1 μM), AC220 (20nM), or the combination for 8 hr were analyzed for FLT3 and phosphotyrosine (pY) by western blotting. Input lysates were analyzed for p-STAT5, STAT5, and β-actin.

(C) FLT-ITD AML CD34$^+$ cells with or without prior nutlin-3 (5 μM) exposure for 2 hr were exposed to TV6 (1 μM), AC220 (20nM), or the combination for 8 hr and analyzed for acetylated p53 (K382), total p53, SIRT1, p-STAT5, STAT5, and β-actin by western blotting.

(D) p53 target gene expression in FLT3-ITD AML CD34$^+$ cells treated with TV6 and AC220 compared with AC220 alone (n = 7)

(E and F) FLT3-ITD AML CD34$^+$ (n = 11) cells were treated with TV6, AC220, or the combination for 48 hr. (E) Cell survival was analyzed by annexin V labeling. (F) Cell growth was evaluated using the CellTiter-Glo assay.

(legend continued on next page)

protein phosphorylation (Marshall et al., 2011; Menssen et al., 2012). SIRT1 knockdown or TV6 treatment increased c-MYC acetylation in FLT3-ITD AML cells, more readily detectable after inhibition of class I and II histone deacetylase activity by Trichostatin A (Figures S6D and S6E) (Vaziri et al., 2001). SIRT1 knockdown or TV6 also reduced c-MYC Ser62 phosphorylation in FLT3-ITD AML CD34$^+$ cells, with further reduction seen in combination with AC220 (Figures S6B and S6F). Both ShSIRT1 and TV6 reduced c-MYC protein levels (Figures 6E, S6B, S6D, and S6F) and c-MYC transcriptional activity (Figure S6G; data not shown). Consistent with a potential role for SIRT1 in regulation of c-MYC stability, TV6 reduced the half-life of c-MYC protein in CHX-treated cells while increasing the half-life of p53 (Figure S6H). The combination of AC220 with ShSIRT1 or TV6 further reduced c-MYC expression and activity (Figures 6E, S6B, S6F, and S6G). These observations suggest that SIRT1-mediated deacetylation leads to enhanced c-MYC protein stability, expression, and activity. Our results support the existence of a positive feedback loop in which c-MYC and SIRT1 increase each other's expression and activity in FLT3-ITD AML cells, which could contribute to partial maintenance of MYC activity after AC220 treatment.

USP22 Interacts with SIRT1 and Maintains Its Protein Expression

The USP22 deubiquitinase has been reported to stabilize SIRT1 by removing polyubiquitin chains conjugated on to SIRT1 (Lin et al., 2012). USP22 mRNA expression was significantly higher in FLT3-ITD compared to FLT3-WT AML CD34$^+$ cells (Figure 7A). Lentiviral expression of FLT3-ITD in CB CD34$^+$ cells resulted in increased USP22 expression compared to FLT3-WT or vector controls (Figure 7B). Knockdown of endogenous USP22 in MV4-11 cells decreased SIRT1 protein levels (Figure 7C) and significantly reduced cell growth (Figure S7A). The proteasome inhibitor MG132 or PS341 restored SIRT1 expression in USP22 knockdown cells (Figure 7C). Ectopic USP22 expression increased SIRT1 protein levels (Figure 7D) without significantly affecting SIRT1 mRNA level (data not shown). The half-life of SIRT1 protein was increased in USP22-overexpressing cells compared to control cells (Figure 7E). AC220 treatment only marginally affected USP22 protein expression in MV4-11 cells (Figures S7B and S7C). USP22 coimmunoprecipitated with SIRT1 (Figure S7B), and this association was not significantly affected by AC220 treatment (Figure S7B). These results indicate that USP22 directly interacts with SIRT1 and contributes to stabilization of SIRT1 protein in FLT3-ITD AML cells.

We further evaluated the contribution of USP22 to c-MYC-mediated reduction in SIRT1 ubiquitination and degradation. Knockdown of c-MYC expression reduced USP22 protein levels in MV4-11 cells (Figure 7F), whereas ectopic expression of c-MYC in CD34$^+$ or HEK293 cells increased USP22 protein levels (Figures 7G and S7D). It is interesting that c-MYC overexpression or knockdown did not affect USP22 mRNA levels (Figures S7E and S7F), indicating that MYC may regulate USP22 posttranscriptionally. It is also interesting that downregulation of SIRT1 expression following c-MYC knockdown was prevented, at least in part, by USP22 overexpression (Figure 7H). In addition, USP22 knockdown prevented c-MYC-mediated reduction of SIRT1 ubiquitination (Figure 7I) and increase in SIRT1 expression (Figure S7G). These results support a role for USP22 in MYC-mediated increase in SIRT1 protein stabilization.

DISCUSSION

We have found that AML stem/progenitor cells demonstrate varying levels of SIRT1 overexpression and sensitivity to SIRT1 inhibitor treatment. The FLT3-ITD mutation was a major determinant of sensitivity to SIRT1 inhibition. FLT3-ITD AML stem/progenitor cells demonstrated high SIRT1 protein levels and sensitivity to SIRT1 inhibition both in vitro and in vivo. The effects of SIRT1 inhibition on FLT3-ITD AML cells were related to increased p53 acetylation and transcriptional activity. These results indicate an important role for SIRT1-mediated downregulation of p53 in growth and maintenance of FLT3-ITD AML LSCs. SIRT1 inhibition only modestly inhibited proliferation of normal CD34$^+$ cells without significantly altering their survival, indicating relative selectivity for AML LSCs. The combination of SIRT1 inhibition with the FLT3 TKI AC220 significantly enhanced targeting of FLT3-ITD AML progenitors in vitro and FLT3-ITD AML LSCs in vivo compared to AC220 alone, indicating that SIRT1 activation contributes to therapeutic resistance of FLT3-ITD AML LSCs.

Increased SIRT1 protein expression in FLT3-ITD AML stem/progenitor cells was related to increased protein half-life. AC220 treatment partially inhibited SIRT1 expression in FLT3-ITD$^+$ cells. Our studies indicate a potential role for c-MYC in SIRT1 regulation in FLT3-ITD cells. Our analysis of public microarray data sets show significant enrichment of c-MYC-related genes in FLT3-ITD compared to FLT3-WT AML cells, confirming previous reports of increased c-MYC in FLT3-ITD AML cells (Kim et al., 2007). c-MYC can potentially modulate SIRT1 activity by increasing NAD+ levels through NAMPT gene induction or by sequestering the SIRT1 inhibitor DBC-1 (Menssen et al., 2012). We identified a mechanism of c-MYC regulation of SIRT1 protein expression by reduction of SIRT1 polyubiquitination and proteasomal degradation. AC220 reduced c-MYC Ser62 phosphorylation and expression in FLT3-ITD cells, indicating that increased c-MYC was at least partially dependent on FLT3 kinase activity. Our results suggest that enhanced c-MYC phosphorylation and expression is related to activation of the PIM-1 kinase downstream of FLT3-ITD (Choudhary et al., 2009; Yang et al., 2012). SIRT1 is known to interact with and deacetylate c-MYC, but the functional consequences of c-MYC deacetylation are unclear. Several groups have reported that c-MYC or N-MYC

(G) FLT3-ITD AML CD34$^+$ cells (n = 4) exposed to TV-6 or AC220 and combination were plated in methylcellulose progenitor culture, and erythrocytic and granulocytic colonies were enumerated after 14 days.
(H–J) FLT3-ITD AML (n = 4) CD34$^+$ cells transduced with control shRNA (Ctrl ShRNA) and ShSIRT1 vectors were cultured with or without AC220 (20 nM) for 72 hr. (H) Cell survival was analyzed by annexin V labeling. (I) Cell growth was evaluated using the CellTiter-Glo assay. (J) Clonogenic assays were performed, and erythrocytic and granulocytic colonies were enumerated after 14 days.
Cumulative results represent the mean ± SEM. *$p < 0.05$ and **$p < 0.01$, compared with indicated groups. See also Figure S4.

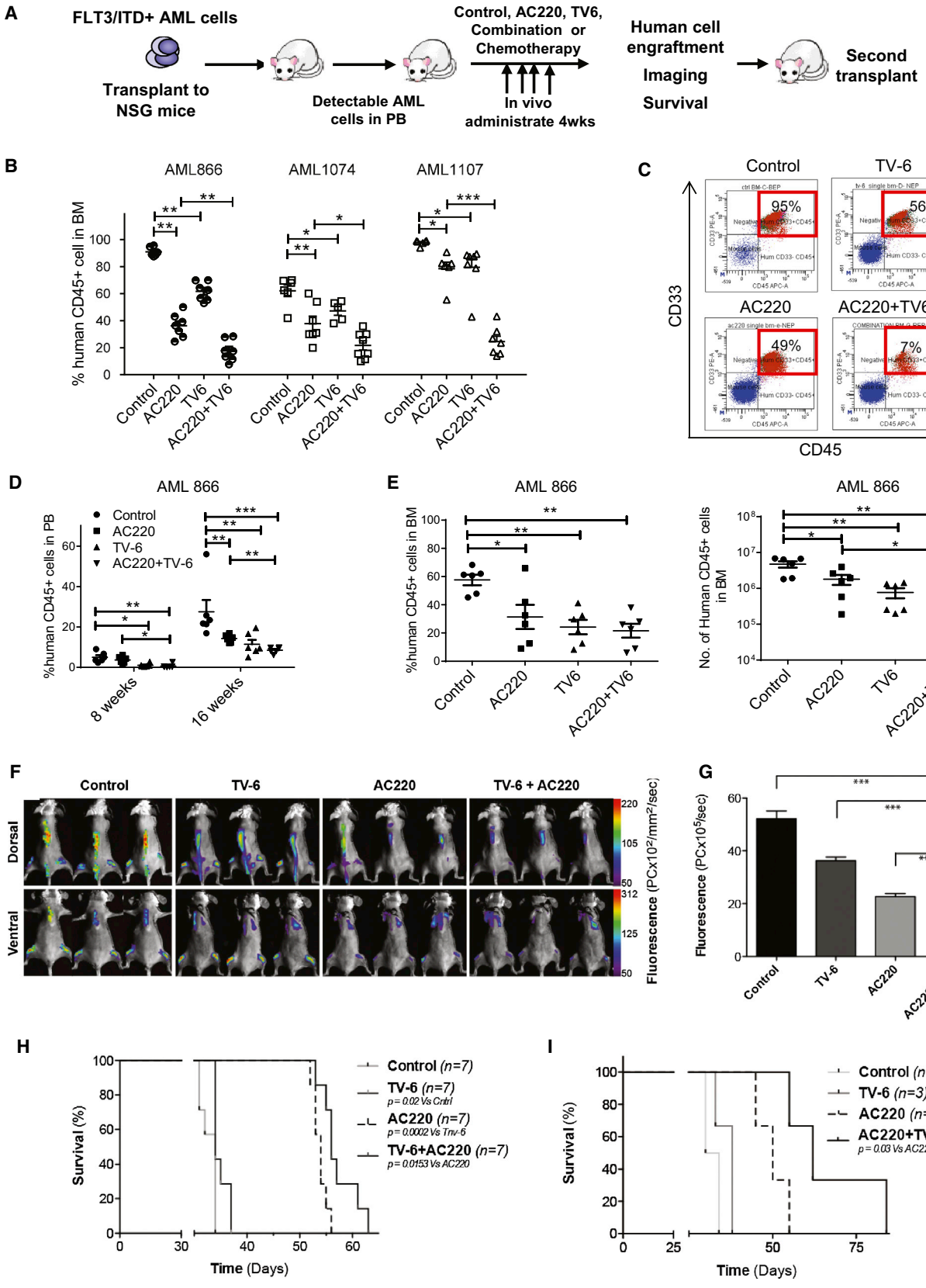

(legend on next page)

deacetylation by SIRT1 leads to increased stability and activity through multiple mechanisms, including altered ubiquitination, altered phosphorylation via reduced MKP3 expression (Marshall et al., 2011), and increased c-MYC-MAX heterodimerization (Menssen et al., 2012), whereas one study found that SIRT1 reduced c-MYC stability and function (Yuan et al., 2009). We found that SIRT1 inhibition resulted in increased c-MYC acetylation, reduced c-MYC phosphorylation, enhanced c-MYC degradation, and reduced c-MYC expression and activity in FLT3-ITD cells. Our results suggest that a feed-forward SIRT1-c-MYC activation loop in FLT3-ITD AML, with reciprocal activation of SIRT1 and c-MYC by each other, may contribute to the maintenance of c-MYC activity in TKI-treated cells.

The USP22 deubiquitinase is reported to complex with SIRT1 and act as a SIRT1 deubiquitinase. USP22 is part of a death-from-cancer gene signature (Zhang et al., 2008) associated with poor prognosis in a variety of cancers (Schrecengost et al., 2014). To date, it is known to be part of the SAGA complex required for c-MYC-related transformation (Zhang et al., 2008). USP22 expression was significantly increased in FLT3-ITD AML $CD34^+$ cells and was marginally affected by blocking FLT3 kinase activity. We show an important role for c-MYC in upregulation of USP22 protein expression in FLT3-ITD cells. However, although USP22 mRNA expression was increased in FLT3-ITD AML cells, it was not increased following MYC overexpression, indicating that additional MYC-independent mechanisms may contribute to increased USP22 transcription. Previous reports showed divergent effects of USP22 on SIRT1 levels (Lin et al., 2012; Armour et al., 2013). We show that USP22 directly interacts with SIRT1 in FLT3-ITD AML cells in a FLT3-kinase-independent manner. USP22 knockdown reduced SIRT1 expression in FLT3-ITD AML cells, whereas USP22 overexpression increased SIRT1 levels by increasing protein stability, indicating that USP22 is an important positive regulator of SIRT1 in FLT3-ITD cells. We further show that USP22 plays an important role in mediating c-MYC-driven inhibition of SIRT1 ubiquitination and degradation. These findings elucidate a mechanistic connection between FLT3, c-MYC, and USP22 in the regulation of SIRT1 in FLT3-ITD AML cells.

SIRT1 overexpression was associated with down-modulation of p53 activity in FLT3-ITD AML $CD34^+$ cells. SIRT1 can negatively regulate p53 by deacetylating several lysine sites (Vaziri et al., 2001; Brooks and Gu, 2009). Acetylation of p53 modulates protein stability and transcriptional activity independent of phosphorylation status (Tang et al., 2008). It is interesting that SIRT1 inhibition did not effectively induce p53 activation or inhibit FLT3-WT AML cells, despite their having nonmutated p53, whereas MDM2 inhibitors such as nutlin-3 could activate p53 in FLT3-WT AML cells and even normal cells (Shangary et al., 2008). SIRT1 overexpression may be necessary to inhibit p53 activity and allow maintenance of AML cells in the setting of FLT3-ITD-induced oncogenic stress, similar to its potential role as an adaptive response to BCR-ABL-related oncogenic stress in CML cells (Li et al., 2012). In contrast SIRT1 activation was not a feature of AML cells with FLT3-TKD mutations, which may have different signaling and transformative properties compared to FLT3-ITD mutations (Kindler et al., 2010). Further studies are required to determine the spectrum and nature of oncogenic stimuli that induce SIRT1 activation and sensitivity to SIRT1 inhibition. In addition to p53, SIRT1 can also deacetylate several other proteins that regulate cell growth and survival (Brooks and Gu, 2009). Indeed, our studies show the importance of SIRT1 regulation of c-MYC in FLT3-ITD AML cells. The role of additional SIRT1 targets such as Ku70 (Yuan et al., 2012; Wang et al., 2013) in LSC transformation and drug resistance requires further investigation.

Our results show the importance of identifying subgroups of patients that could benefit from SIRT1 inhibitor treatment, given the heterogeneous genetic background of leukemias such as AML. Our results are consistent with those of Bradbury et al. (2005), who observed increased SIRT1 expression in most AML samples. In contrast, Dan et al. (2012) found that SIRT1 mRNA was unchanged or even slightly diminished in AML blasts, compared with normal $CD34^+$, cells but did not determine association with AML subtypes. In addition, these studies did not evaluate protein levels, which we show here to be critically important. Another study from Sasca et al. (2014), published while this paper was under review, also reported SIRT1 protein overexpression in FLT3-ITD AML samples. Leukemic blasts from murine AML models based on coexpression of MLL-AF9 or AML1-ETO with FLT3-ITD showed dependence on SIRT1 activity. Although in vivo analysis of primary human AML LSC was not performed, the results of this study are consistent with our own and support SIRT1 inhibition as an attractive therapeutic

Figure 5. SIRT1 Inhibition Reduces In Vivo Growth of Primary AML Stem Cells in Immunodeficient Mice

(A) T-depleted primary human AML cells were injected into NSG mice (2×10^6 cells per mouse). After engraftment was confirmed, mice were treated for 4 weeks with AC220 (10 mg/kg/day, oral gavage), TV6 (100 mg/kg/day intraperitoneally), the combination of TV6 and AC220, or vehicle (controls) (n = 7 or 8 mice per group). Engraftment of human cells was analyzed by flow cytometry. Imaging, secondary transplantation, and survival analysis were also performed.

(B) The percentage of human AML $CD45^+$ cells from three different samples (AML 866, AML 1074, and AML 1107) in the BM of treated mice.

(C) Representative results for CD45 and CD33 expression from AML 866.

(D) The percentage of human AML $CD45^+$ cells (AML866) in blood of secondary recipients of BM cells from treated mice (2×10^6 cells per mouse, n = 6 per group) at 8 and 16 weeks.

(E) The percentage and number of human AML $CD45^+$ cells (AML 866) in the BM of secondary recipient mice at 16 weeks.

(F) $CD34^+$ cells from a chemotherapy-resistant FLT3-ITD AML patient were injected into NSG mice and treated for 4 weeks (n = 10 per group) with vehicle, AC220, TV6, or the combination. Subsequently, three mice from each group were injected with fluorescently labeled monoclonal antibodies and imaged by time domain optical imaging. PC, photon counts.

(G) Quantitative results from bioimaging studies analyzed by Optiview software (Version 3.03, ART). Results represent mean ± SEM for three mice. $^*p < 0.05$, $^{**}p < 0.01$, and $^{***}p < 0.001$, compared with combination.

(H) Survival of mice from (F) after discontinuation of treatment. PC, photon counts.

(I) Survival after transplantation of BM cells from treated mice (F) into secondary recipients.

For (B), (D), and (E), results represent the mean ± SEM. $^*p < 0.05$, $^{**}p < 0.01$, and $^{***}p < 0.001$; comparison has been indicated in the graph. See also Figure S5.

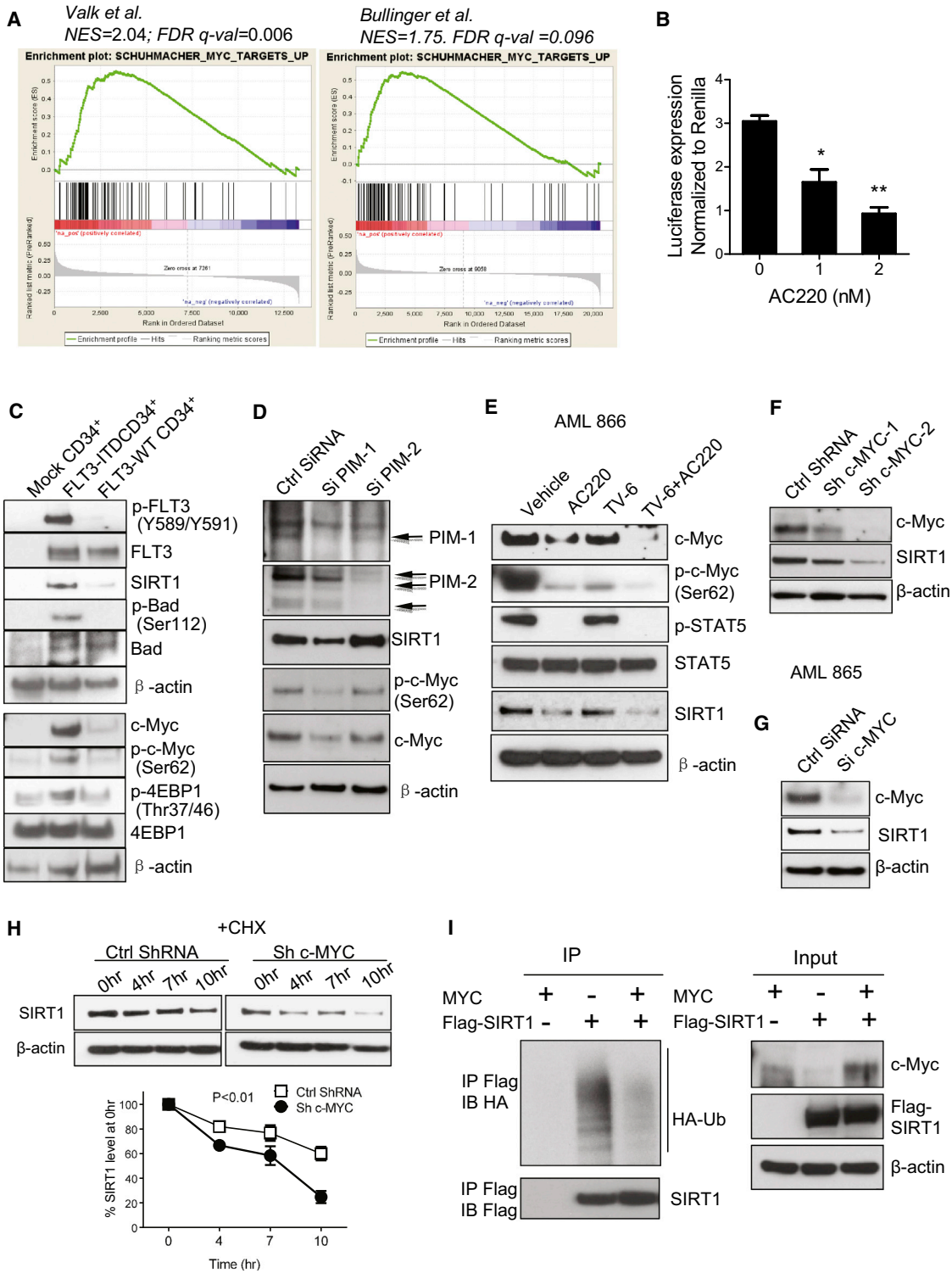

Figure 6. Cross-Regulation of SIRT1 and MYC in FLT3-ITD AML Cells

(A) Gene set enrichment analysis showing enrichment of a MYC gene set (Schuhmacher et al., 2001) in FLT3-ITD versus FLT3-WT AML cells in two large microarray data sets. Normalized enrichment score (NES) and statistical significance/false discovery rate q value (FDR q val) are indicated.

(B) MV4-11 cells cotransfected with a c-MYC firefly luciferase reporter and a Renilla luciferase plasmid were exposed with AC220 or vehicle control for 24 hr and assayed for luciferase normalized to Renilla activity. The mean value of triplicate experiments is shown.

(C) Western blotting for SIRT1, FLT3, pFLT3 (Y589/Y591), p-Bad (ser112), Bad, p-4EBP1 (Thr37/46), 4EBP1, p-c-MYC (ser62), c-MYC, and β-actin in CB CD34$^+$ cells transduced with FUGW, FUGW/FLT3-ITD, or FUGW/FLT3-WT vectors.

(legend continued on next page)

strategy in FLT3-ITD AML. The selectivity of SIRT1 inhibition toward FLT3-ITD AML cells is expected to yield a high therapeutic index toward leukemic cells. Small molecule SIRT1 inhibitors are being investigated as potential anticancer treatments (Alcaín and Villalba, 2009). Although the pharmacological properties of TV6 may not allow it to be a suitable candidate for drug development, it is a useful compound to study potential therapeutic effects of SIRT1 inhibition in cancer. Our observations support further investigation of Tenovin derivatives and other SIRT1 inhibitors to target FLT3-ITD AML, in combination with TKI treatment.

In conclusion, this study improves our understanding of mechanisms underlying the function of SIRT1 as an oncogene versus tumor suppressor gene in specific genetic contexts; elucidates a mechanistic connection between FLT3, c-MYC, and USP22 in regulation of SIRT1 and p53, and supports further development of SIRT1 inhibition as a potential approach for more selective targeting of malignant stem cells in selected cancers.

EXPERIMENTAL PROCEDURES

Samples and Materials

PB or BM samples were obtained from AML patients with active disease at diagnosis or at relapse in two centers. Patient characteristics are shown in Tables S1 and S2. Risk groups were based on NCCN criteria (Table S3) (O'Donnell et al., 2012). Normal PBSCs were obtained from allogeneic transplant donors. CB was obtained from StemCyte. All subjects signed informed consent forms. Sample acquisition was approved by the City of Hope (COH) Institutional Review Board or the regional Ethics Committee (REK Vest; http://helseforskning.etikkom.no; Norwegian Ministry of Education and Research) in accordance with the Declaration of Helsinki. Mononuclear cells were isolated by Ficoll-Hypaque (Sigma Diagnostics) centrifugation. $CD34^+$ cells or $CD3^-$ cells were selected using immunomagnetic columns (Miltenyi Biotec). Details of cell lines, drugs, and DNA constructs are provided in the Supplemental Experimental Procedures.

Cell Transduction and Transfection

$CD34^+$ cells were transduced with lentivirus vectors expressing shRNA or FLT3 constructs (provided by Dr. Linzhao Cheng, Johns Hopkins University). MV4-11 cells were transduced with PITA-SIRT1-R vectors. Human AML $CD34^+$ cells or MV4-11 cells were transfected with siRNAs to FLT3, c-MYC, BAX, PIM-1, PIM-2, and control siRNAs (Applied BioSystems/Ambion) using the Amaxa Nucleofector. Details are provided in the Supplemental Experimental Procedures.

Intracellular Staining for SIRT1

$CD34^+$ cells were labeled with CD34-PeCy7, Lin-APC-Cy7 (including CD2, CD3, CD7, CD10, CD19, and CD235a), and CD38-APC or CD38-PE, CD90-PercpCy5.5, CD123-APC, or CD47-APC (eBioscience) antibodies; fixed and permeabilized (Cytofix/Cytoperm Kit, Beckman Coulter); labeled with rabbit anti-human SIRT1 (E1104-1, Millipore) and Alexa Fluor 488-conjugated goat anti-rabbit antibodies (Invitrogen); and analyzed by flow cytometry. Data were analyzed using FlowJo software (version 8.5.2; TreeStar).

Analysis of Viability and Growth

Cells were labeled with annexin V/DAPI, and the percentage of surviving cells (Annexin V^- $DAPI^-$) was analyzed. Cell viability was also assessed by Hoechst 33342 staining (Invitrogen). Cell growth was evaluated using the CellTiter-Glo assay (Promega). Details are provided in the Supplemental Experimental Procedures.

In Vivo Treatment of AML-Engrafted Immunodeficient Mice

T-cell-depleted or $CD34^+$ selected human AML cells were transplanted into sublethally irradiated (300 cGy) 8-week-old NOD.Cg-Prkdcscid IL2rgtm1Wjl/SzJ mice (NSG mice, Jackson Laboratory). After engraftment was confirmed, mice were treated with AC220, TV6, the combination, or vehicle for 4 weeks or with chemotherapy as described elsewhere (McCormack et al., 2013). BM, PB, and spleen cells were analyzed for engraftment by flow cytometry analysis of human $CD45^+$ cells. A group of mice was followed for survival after discontinuation of treatment. BM cells from primary recipients were used for secondary transplantation into irradiated NSG mice (2×10^6 cells per mouse), and engraftment was analyzed after 16 weeks. The procedure for evaluation of engraftment, the luciferase-expressing MOLM-13 xenograft model, and optical imaging are described elsewhere (McCormack et al., 2012) details of which can also be found in the Supplemental Experimental Procedures. Mouse care and experimental procedures were performed in accordance with approved protocols from the Institutional Animal Care and Use Committee at the COH National Medical Center and Norwegian Animal Research Authority in accordance with The European Convention for the Protection of Vertebrates Used for Scientific Purposes.

Luciferase Reporter Assays

MV4-11 cells were transduced with c-Myc reporter (Cignal Myc Lentivirus Reporter, QIAGEN) and selected for Puro resistance. Reporter activity was measured by the Dual-Glo Luciferase Assay System (Promega) and normalized to EF1α-renilla luciferase.

Real-Time Quantitative PCR Analysis

Real-time quantitative PCR analysis was performed with primers and probes for *p21*, *BAX*, *PUMA*, *NOXA*, *DR5*, *USP22*, and *SIRT1*. Details are provided in the Supplemental Experimental Procedures.

Immunoprecipitation and Western Blotting

Antibodies used for immunoprecipitation were conjugated with Flag/M2 beads (Sigma-Aldrich) or protein A/G beads using an antibody crosslinking kit (Pierce Biotechnology). Western blotting was performed as described in the Supplemental Experimental Procedures.

Statistics

Data obtained from independent experiments were reported as the mean ± SEM. Student's t test, Mann-Whitney test, and two-way ANOVA with multiple testing were performed to determine statistical significance as appropriate. $p < 0.05$ was considered statistically significant.

(D) Western blotting for PIM-1, PIM-2, SIRT, p-c-MYC (Ser62), c-MYC, and β-actin in control siRNA (Ctrl SiRNA)-, PIM-1- or PIM-2-siRNA-transfected MV4-11 cells.

(E) Cells cultured with TV6 (1 μM), AC220 (20 nM), or the combination for 8 hr were analyzed by western blotting for SIRT1, c-MYC, p-c-MYC (Ser62), β-actin, p-STAT5, and STAT5.

(F) Western blotting for SIRT1 and c-MYC levels in c-MYC-shRNA-expressing MV4-11 cells.

(G) Western blotting for SIRT1 and c-MYC levels following siRNA-mediated c-MYC knockdown in FLT3-ITD AML $CD34^+$ cells.

(H) Western blotting for SIRT1 following CHX treatment of c-MYC knockdown or control MV4-11 cells (upper panel). The lower panel shows results of densitometry quantitation (n = 3).

(I) HEK293 cells were cotransfected with Flag-SIRT1 or vector control, c-MYC or empty vector control, and HA-tagged ubiquitin (Ub) as indicated; then lysates were immunoprecipitated (IP) for Flag and western blotted for SIRT1, c-MYC, and HA. The right panel shows input levels based on western blotting of lysates for SIRT1, c-MYC, and β-actin. IB, immunoblotting.

For (B) and (H), results represent mean ± SEM from three independent experiments. *$p < 0.05$, **$p < 0.01$, and ***$p < 0.001$; comparison has been made to no drug control (B) or control shRNA (H). See also Figure S6.

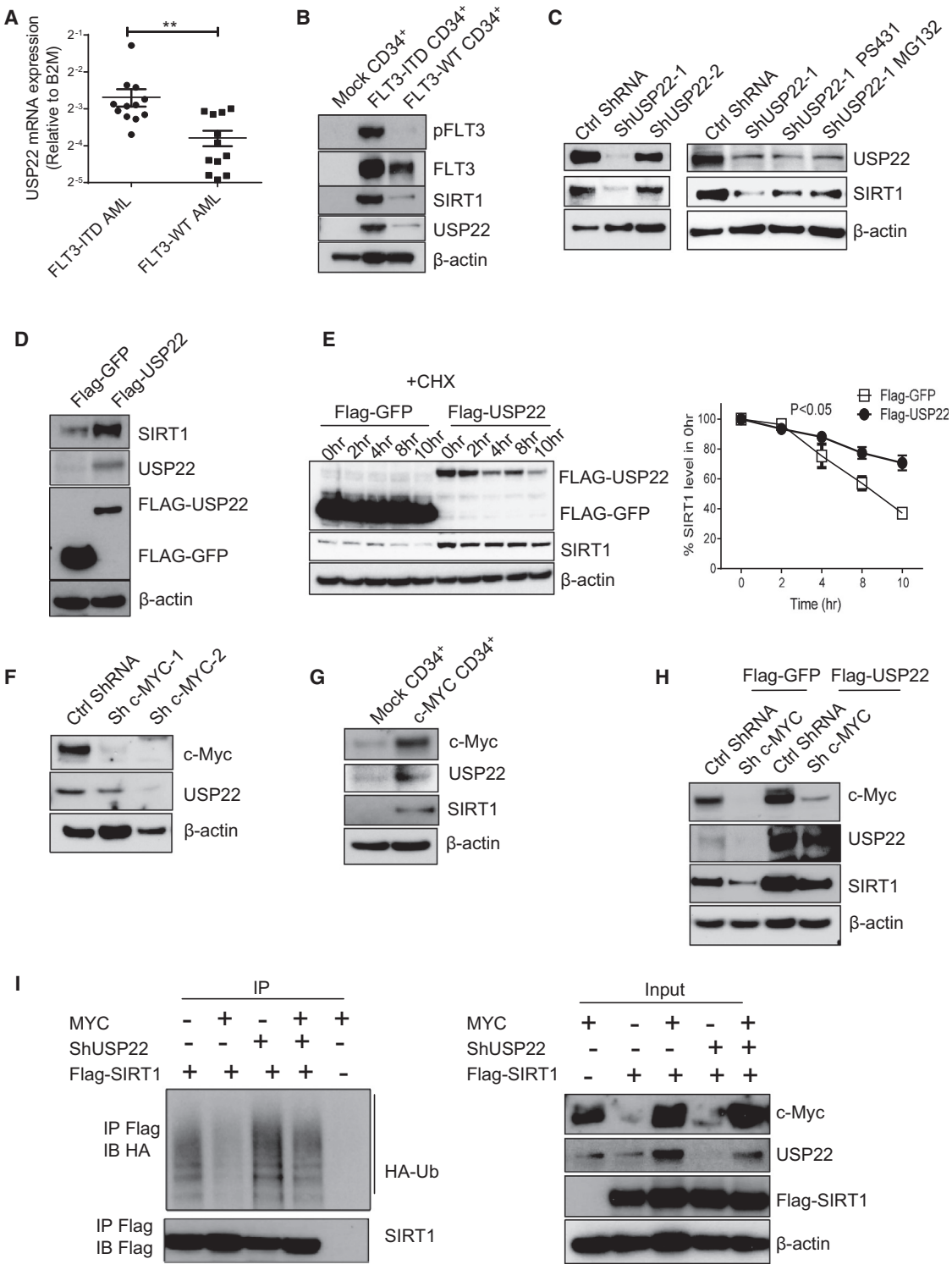

Figure 7. USP22 Interacts with SIRT1 and Maintains Its Protein Expression

(A) USP22 mRNA levels in FLT3-ITD (n = 12) and FLT3-WT (n = 12) AML $CD34^+$ cells.

(B) Western blotting for SIRT1, FLT3, pFLT3 (Y589/Y591), USP22, and β-actin in CB $CD34^+$ cells transduced with FUGW, FUGW/FLT3-ITD, or FUGW/FLT3-WT vectors.

(C) Western blotting for SIRT1, USP22, and β-actin expression in MV4-11 cells expressing shRNA to USP22 or control shRNA (Ctrl ShRNA) (left panel). Western blotting for SIRT1, USP22, and β-actin was also performed on shRNA-expressing cells incubated with MG132 (10 μM) or PS341 (50 nM) for 4 hr (right panel).

(D) Western blotting for SIRT1, USP22, Flag, and β-actin in MV4-11 cells transfected with Flag-GFP or Flag-USP22.

(legend continued on next page)

SUPPLEMENTAL INFORMATION

Supplemental Information for this article includes Supplemental Experimental Procedures, seven figures, and three tables and can be found with this article online at http://dx.doi.org/10.1016/j.stem.2014.08.001.

ACKNOWLEDGMENTS

This work was supported by National Cancer Institute grants R01 CA95684, P30CA033572, and K99CA184411; the Leukemia and Lymphoma Society; the Bergen Research Foundation; the Norwegian Cancer Society; and the Western Norway Regional Health Authority. We thank StemCyte for CB samples. We thank Linda Seymour and Vincent Paterno for sample acquisition; Xiwei Wu for microarray analysis; the COH Analytical Cytometry Core Facility; and Line Wergeland, Michael Sæterhaug, Sahba Shafiee, Zina Fandalyuk, and Ingvild Haaland for assistance in cell viability assays and preclinical studies. All imaging was conducted at the Molecular Imaging Center, the Department of Biomedicine, University of Bergen.

Received: February 4, 2014
Revised: July 11, 2014
Accepted: August 8, 2014
Published: October 2, 2014

REFERENCES

Alcaín, F.J., and Villalba, J.M. (2009). Sirtuin inhibitors. Expert Opin. Ther. Pat. *19*, 283–294.

Armour, S.M., Bennett, E.J., Braun, C.R., Zhang, X.Y., McMahon, S.B., Gygi, S.P., Harper, J.W., and Sinclair, D.A. (2013). A high-confidence interaction map identifies SIRT1 as a mediator of acetylation of USP22 and the SAGA coactivator complex. Mol. Cell. Biol. *33*, 1487–1502.

Bradbury, C.A., Khanim, F.L., Hayden, R., Bunce, C.M., White, D.A., Drayson, M.T., Craddock, C., and Turner, B.M. (2005). Histone deacetylases in acute myeloid leukaemia show a distinctive pattern of expression that changes selectively in response to deacetylase inhibitors. Leukemia *19*, 1751–1759.

Brooks, C.L., and Gu, W. (2009). How does SIRT1 affect metabolism, senescence and cancer? Nat. Rev. Cancer *9*, 123–128.

Bullinger, L., Döhner, K., Kranz, R., Stirner, C., Fröhling, S., Scholl, C., Kim, Y.H., Schlenk, R.F., Tibshirani, R., Döhner, H., and Pollack, J.R. (2008). An FLT3 gene-expression signature predicts clinical outcome in normal karyotype AML. Blood *111*, 4490–4495.

Choudhary, C., Olsen, J.V., Brandts, C., Cox, J., Reddy, P.N., Böhmer, F.D., Gerke, V., Schmidt-Arras, D.E., Berdel, W.E., Müller-Tidow, C., et al. (2009). Mislocalized activation of oncogenic RTKs switches downstream signaling outcomes. Mol. Cell *36*, 326–339.

Chu, S.H., Heiser, D., Li, L., Kaplan, I., Collector, M., Huso, D., Sharkis, S.J., Civin, C., and Small, D. (2012). FLT3-ITD knockin impairs hematopoietic stem cell quiescence/homeostasis, leading to myeloproliferative neoplasm. Cell Stem Cell *11*, 346–358.

Dan, L., Klimenkova, O., Klimiankou, M., Klusman, J.H., van den Heuvel-Eibrink, M.M., Reinhardt, D., Welte, K., and Skokowa, J. (2012). The role of sirtuin 2 activation by nicotinamide phosphoribosyltransferase in the aberrant proliferation and survival of myeloid leukemia cells. Haematologica *97*, 551–559.

Eppert, K., Takenaka, K., Lechman, E.R., Waldron, L., Nilsson, B., van Galen, P., Metzeler, K.H., Poeppl, A., Ling, V., Beyene, J., et al. (2011). Stem cell gene expression programs influence clinical outcome in human leukemia. Nat. Med. *17*, 1086–1093.

Han, M.K., Song, E.K., Guo, Y., Ou, X., Mantel, C., and Broxmeyer, H.E. (2008). SIRT1 regulates apoptosis and Nanog expression in mouse embryonic stem cells by controlling p53 subcellular localization. Cell Stem Cell *2*, 241–251.

Horton, S.J., and Huntly, B.J. (2012). Recent advances in acute myeloid leukemia stem cell biology. Haematologica *97*, 966–974.

Jordan, C.T., Upchurch, D., Szilvassy, S.J., Guzman, M.L., Howard, D.S., Pettigrew, A.L., Meyerrose, T., Rossi, R., Grimes, B., Rizzieri, D.A., et al. (2000). The interleukin-3 receptor alpha chain is a unique marker for human acute myelogenous leukemia stem cells. Leukemia *14*, 1777–1784.

Kim, K.T., Baird, K., Davis, S., Piloto, O., Levis, M., Li, L., Chen, P., Meltzer, P., and Small, D. (2007). Constitutive Fms-like tyrosine kinase 3 activation results in specific changes in gene expression in myeloid leukaemic cells. Br. J. Haematol. *138*, 603–615.

Kindler, T., Lipka, D.B., and Fischer, T. (2010). FLT3 as a therapeutic target in AML: still challenging after all these years. Blood *116*, 5089–5102.

Leko, V., Varnum-Finney, B., Li, H., Gu, Y., Flowers, D., Nourigat, C., Bernstein, I.D., and Bedalov, A. (2012). SIRT1 is dispensable for function of hematopoietic stem cells in adult mice. Blood *119*, 1856–1860.

Levis, M. (2011). FLT3/ITD AML and the law of unintended consequences. Blood *117*, 6987–6990.

Li, L., Wang, L., Li, L., Wang, Z., Ho, Y., McDonald, T., Holyoake, T.L., Chen, W., and Bhatia, R. (2012). Activation of p53 by SIRT1 inhibition enhances elimination of CML leukemia stem cells in combination with imatinib. Cancer Cell *21*, 266–281.

Lin, Z., Yang, H., Kong, Q., Li, J., Lee, S.M., Gao, B., Dong, H., Wei, J., Song, J., Zhang, D.D., and Fang, D. (2012). USP22 antagonizes p53 transcriptional activation by deubiquitinating Sirt1 to suppress cell apoptosis and is required for mouse embryonic development. Mol. Cell *46*, 484–494.

Long, J., Parkin, B., Ouillette, P., Bixby, D., Shedden, K., Erba, H., Wang, S., and Malek, S.N. (2010). Multiple distinct molecular mechanisms influence sensitivity and resistance to MDM2 inhibitors in adult acute myelogenous leukemia. Blood *116*, 71–80.

MacCallum, S.F., Groves, M.J., James, J., Murray, K., Appleyard, V., Prescott, A.R., Drbal, A.A., Nicolaou, A., Cunningham, J., Haydock, S., et al. (2013). Dysregulation of autophagy in chronic lymphocytic leukemia with the small-molecule Sirtuin inhibitor Tenovin-6. Sci. Rep. *3*, 1275.

Majeti, R., Chao, M.P., Alizadeh, A.A., Pang, W.W., Jaiswal, S., Gibbs, K.D., Jr., van Rooijen, N., and Weissman, I.L. (2009). CD47 is an adverse prognostic factor and therapeutic antibody target on human acute myeloid leukemia stem cells. Cell *138*, 286–299.

Marshall, G.M., Liu, P.Y., Gherardi, S., Scarlett, C.J., Bedalov, A., Xu, N., Iraci, N., Valli, E., Ling, D., Thomas, W., et al. (2011). SIRT1 promotes N-Myc oncogenesis through a positive feedback loop involving the effects of MKP3 and ERK on N-Myc protein stability. PLoS Genet. *7*, e1002135.

McCormack, E., Haaland, I., Venås, G., Forthun, R.B., Huseby, S., Gausdal, G., Knappskog, S., Micklem, D.R., Lorens, J.B., Bruserud, O., and Gjertsen, B.T. (2012). Synergistic induction of p53 mediated apoptosis by valproic acid and nutlin-3 in acute myeloid leukemia. Leukemia *26*, 910–917.

(E) Flag-USP22-expressing or control MV4-11 cells were incubated with CHX and analyzed by western blotting for Flag, SIRT1, and β-actin. The right panel indicates the relative amount of SIRT1 analyzed by densitometry from three experiments.
(F) Western blotting for c-MYC, USP22, and β-actin in MV4-11 cells expressing shRNA to c-MYC or Ctrl ShRNA.
(G) Western blotting for SIRT1, c-MYC, USP22, and β-actin in CB $CD34^+$ cells transduced with lentivirus vectors expressing c-MYC or vector control.
(H) Western blotting for SIRT1, c-MYC, USP22, and β-actin in Flag-USP22 expressing or control MV4-11 cells expressing c-MYC or Ctrl ShRNA.
(I) HEK293 cells transduced with lentivirus vectors expressing USP22 or Ctrl ShRNA were cotransfected with Flag-SIRT1 or vector control, c-MYC or empty vector control, and HA-tagged ubiquitin (Ub), as indicated, and lysates were immunoprecipitated (IP) for Flag and western blotted for SIRT1, c-MYC, and HA. The right panel shows input lysates for western blotting of SIRT1, c-MYC, USP22, and β-actin. IB, immunoblotting. *$p < 0.05$, **$p < 0.01$, compared with controls. Results represent mean ± SEM and are representative of three independent experiments. See also Figure S7.

McCormack, E., Mujić, M., Osdal, T., Bruserud, Ø., and Gjertsen, B.T. (2013). Multiplexed mAbs: a new strategy in preclinical time-domain imaging of acute myeloid leukemia. Blood *121*, e34–e42.

Menssen, A., Hydbring, P., Kapelle, K., Vervoorts, J., Diebold, J., Lüscher, B., Larsson, L.G., and Hermeking, H. (2012). The c-MYC oncoprotein, the NAMPT enzyme, the SIRT1-inhibitor DBC1, and the SIRT1 deacetylase form a positive feedback loop. Proc. Natl. Acad. Sci. USA *109*, E187–E196.

Nakao, M., Yokota, S., Iwai, T., Kaneko, H., Horiike, S., Kashima, K., Sonoda, Y., Fujimoto, T., and Misawa, S. (1996). Internal tandem duplication of the flt3 gene found in acute myeloid leukemia. Leukemia *10*, 1911–1918.

O'Donnell, M.R., Abboud, C.N., Altman, J., Appelbaum, F.R., Arber, D.A., Attar, E., Borate, U., Coutre, S.E., Damon, L.E., Goorha, S., et al. (2012). Acute myeloid leukemia. J. Natl. Compr. Canc. Netw. *10*, 984–1021.

Ou, X., Chae, H.D., Wang, R.H., Shelley, W.C., Cooper, S., Taylor, T., Kim, Y.J., Deng, C.X., Yoder, M.C., and Broxmeyer, H.E. (2011). SIRT1 deficiency compromises mouse embryonic stem cell hematopoietic differentiation, and embryonic and adult hematopoiesis in the mouse. Blood *117*, 440–450.

Patel, J.P., Gönen, M., Figueroa, M.E., Fernandez, H., Sun, Z., Racevskis, J., Van Vlierberghe, P., Dolgalev, I., Thomas, S., Aminova, O., et al. (2012). Prognostic relevance of integrated genetic profiling in acute myeloid leukemia. N. Engl. J. Med. *366*, 1079–1089.

Sasca, D., Hähnel, P.S., Szybinski, J., Khawaja, K., Kriege, O., Pante, S.V., Bullinger, L., Strand, S., Strand, D., Theobald, M., and Kindler, T. (2014). SIRT1 prevents genotoxic stress-induced p53 activation in acute myeloid leukemia. Blood *124*, 121–133.

Schrecengost, R.S., Dean, J.L., Goodwin, J.F., Schiewer, M.J., Urban, M.W., Stanek, T.J., Sussman, R.T., Hicks, J.L., Birbe, R.C., Draganova-Tacheva, R.A., et al. (2014). USP22 regulates oncogenic signaling pathways to drive lethal cancer progression. Cancer Res. *74*, 272–286.

Schuhmacher, M., Kohlhuber, F., Hölzel, M., Kaiser, C., Burtscher, H., Jarsch, M., Bornkamm, G.W., Laux, G., Polack, A., Weidle, U.H., and Eick, D. (2001). The transcriptional program of a human B cell line in response to Myc. Nucleic Acids Res. *29*, 397–406.

Shangary, S., Qin, D., McEachern, D., Liu, M., Miller, R.S., Qiu, S., Nikolovska-Coleska, Z., Ding, K., Wang, G., Chen, J., et al. (2008). Temporal activation of p53 by a specific MDM2 inhibitor is selectively toxic to tumors and leads to complete tumor growth inhibition. Proc. Natl. Acad. Sci. USA *105*, 3933–3938.

Singh, S.K., Williams, C.A., Klarmann, K., Burkett, S.S., Keller, J.R., and Oberdoerffer, P. (2013). Sirt1 ablation promotes stress-induced loss of epigenetic and genomic hematopoietic stem and progenitor cell maintenance. J. Exp. Med. *210*, 987–1001.

Smith, C.C., Wang, Q., Chin, C.S., Salerno, S., Damon, L.E., Levis, M.J., Perl, A.E., Travers, K.J., Wang, S., Hunt, J.P., et al. (2012). Validation of ITD mutations in FLT3 as a therapeutic target in human acute myeloid leukaemia. Nature *485*, 260–263.

Tang, Y., Zhao, W., Chen, Y., Zhao, Y., and Gu, W. (2008). Acetylation is indispensable for p53 activation. Cell *133*, 612–626.

Valk, P.J., Verhaak, R.G., Beijen, M.A., Erpelinck, C.A., Barjesteh van Waalwijk van Doorn-Khosrovani, S., Boer, J.M., Beverloo, H.B., Moorhouse, M.J., van der Spek, P.J., Löwenberg, B., and Delwel, R. (2004). Prognostically useful gene-expression profiles in acute myeloid leukemia. N. Engl. J. Med. *350*, 1617–1628.

van der Lugt, N.M., Domen, J., Verhoeven, E., Linders, K., van der Gulden, H., Allen, J., and Berns, A. (1995). Proviral tagging in E mu-myc transgenic mice lacking the Pim-1 proto-oncogene leads to compensatory activation of Pim-2. EMBO J. *14*, 2536–2544.

Vaziri, H., Dessain, S.K., Ng Eaton, E., Imai, S.I., Frye, R.A., Pandita, T.K., Guarente, L., and Weinberg, R.A. (2001). hSIR2(SIRT1) functions as an NAD-dependent p53 deacetylase. Cell *107*, 149–159.

Wang, R.H., Sengupta, K., Li, C., Kim, H.S., Cao, L., Xiao, C., Kim, S., Xu, X., Zheng, Y., Chilton, B., et al. (2008a). Impaired DNA damage response, genome instability, and tumorigenesis in SIRT1 mutant mice. Cancer Cell *14*, 312–323.

Wang, R.H., Zheng, Y., Kim, H.S., Xu, X., Cao, L., Luhasen, T., Lee, M.H., Xiao, C., Vassilopoulos, A., Chen, W., et al. (2008b). Interplay among BRCA1, SIRT1, and Survivin during BRCA1-associated tumorigenesis. Mol. Cell *32*, 11–20.

Wang, Z., Yuan, H., Roth, M., Stark, J.M., Bhatia, R., and Chen, W.Y. (2013). SIRT1 deacetylase promotes acquisition of genetic mutations for drug resistance in CML cells. Oncogene *32*, 589–598.

Yang, Q., Chen, L.S., Neelapu, S.S., Miranda, R.N., Medeiros, L.J., and Gandhi, V. (2012). Transcription and translation are primary targets of Pim kinase inhibitor SGI-1776 in mantle cell lymphoma. Blood *120*, 3491–3500.

Yuan, J., Minter-Dykhouse, K., and Lou, Z. (2009). A c-Myc-SIRT1 feedback loop regulates cell growth and transformation. J. Cell Biol. *185*, 203–211.

Yuan, H., Wang, Z., Li, L., Zhang, H., Modi, H., Horne, D., Bhatia, R., and Chen, W. (2012). Activation of stress response gene SIRT1 by BCR-ABL promotes leukemogenesis. Blood *119*, 1904–1914.

Zhang, X.Y., Varthi, M., Sykes, S.M., Phillips, C., Warzecha, C., Zhu, W., Wyce, A., Thorne, A.W., Berger, S.L., and McMahon, S.B. (2008). The putative cancer stem cell marker USP22 is a subunit of the human SAGA complex required for activated transcription and cell-cycle progression. Mol. Cell *29*, 102–111.